

**CHARACTERIZATION OF AUTOMATICALLY RETICULATED
SHAPE MEMORY POLYMER FOAMS**

An Undergraduate Research Scholars Thesis

by

VINCENT DAVID ZABALLA

Submitted to Honors and Undergraduate Research
Texas A&M University
in partial fulfillment of the requirements for the designation as an

UNDERGRADUATE RESEARCH SCHOLAR

Approved by
Research Advisor:

Dr. Duncan Maitland

May 2014

Major: Biomedical Engineering

TABLE OF CONTENTS

	Page
ABSTRACT	1
DEDICATION	3
ACKNOWLEDGEMENTS	4
NOMENCLATURE	5
CHAPTER	
I INTRODUCTION	6
Clinical motivation	7
Biomedical motivation	9
II METHODS	11
Scanning electron microscope imaging of SMP foams	11
SMP foam fabrication, reticulation, and processing	11
Average pore size verification	14
Permeability system testing of SMP foams	14
Volume expansion of SMP foams	15
Characterization of SMP foams by dynamic mechanical analysis testing	17
III RESULTS AND DISCUSSION	18
Bulk SMP foam comparisons	18
SEM images of different degrees of reticulated foams	19
Average pore sizes of tested SMP foams	21
Permeability and form factor	21
Volume expansion of SMP foams	24
DMA results	25
Discussion	26
IV CONCLUSION	28
REFERENCES	30

ABSTRACT

Characterization of Automatically Reticulated Shape Memory Polymer Foams. (May 2014)

Vincent D. Zaballa
Department of Biomedical Engineering
Texas A&M University

Research Advisor: Dr. Duncan Maitland
Department of Biomedical Engineering

Polyurethane shape memory polymer (SMP) foams have been shown to be biocompatible within porcine models and show potential to treat intracranial saccular aneurysms in patients, and use in other medical applications¹. After initial fabrication, SMP foams are closed-celled foams, a property that could potentially slow or inhibit complete healing of an aneurysm, limiting the potential for use of the foam as a medical application or as potential scaffolds for tissue engineering applications. Mechanical reticulation of SMP foams is a process that creates a network of open-celled pores within SMP foam while preserving the backbone framework of the foam². This process provides pathways for fluid diffusion and the accumulation of clotting factors within the bulk volume of the material; a property useful for SMP foams in medical application and potentially for tissue scaffolds. However, reticulation is also an arduous process that requires a significant time investment. An automated mechanical reticulation system will be used in order to process SMP foams at varying degrees of reticulation, the results of which will be characterized. SMP foams will be studied by changing the density of open-celled pores within a unit area of the foam. The goal of this optimization process will be to characterize the porous media properties, mechanical properties, and recovery volumes of SMP foams as a function of

the number of pathways per unit area. Future work will test these relationships *in vivo* and evaluate their effectiveness at occluding intracranial aneurysms.

DEDICATION

This thesis is dedicated to my family, the people who are able to show me love despite miles of separation, my brother, who was more than a brother most of the time, and my mother, who has always been there for me.

ACKNOWLEDGEMENTS

This thesis was made possible due to the help from many people in the Biomedical Device Lab.

Thanks goes to Dr. Maitland, for his patience, understanding, and for trusting me with the project of automating mechanical reticulation, I am a much better engineer because of that project. Also, for pushing me to write this thesis, as so many opportunities have arose from this work.

This work would not have been possible without the help from my mentor, Todd Landsman. From helping me find a lab, to helping me write a thesis, you have helped me out so much and I know I would not be where I am without your help. Thanks bud.

To Jennifer, the person who introduced mechanical reticulation to me, and the rest of the biomedical device lab, for setting a high bar and helping me to try and reach the same heights they have achieved. I am sure everyone in the lab has helped me in this endeavor; therefore, they all deserve many thanks. Special thanks goes to Tony Boyle for taking the time to just talk about my research and for helping me design my experiments, and Landon Nash and Cameron Maher for showing me how to use various lab equipment.

Finally, this thesis was made easier thanks to Jason and Rachael, my fellow undergraduate researchers, who helped in editing and provided insights for writing this thesis.

NOMENCLATURE

SMPs	Shape Memory Polymers
T _g	Glass Transition Temperature
DMA	Dynamic Mechanical Analysis
SEM	Scanning Electron Microscopy

CHAPTER I

INTRODUCTION

The goal of this research is to characterize shape memory polymer (SMP) foams that have been reticulated to a certain degree using an automatic reticulation system. SMP foams show promise for use as endovascular devices, due to their foamy nature and ability to occlude neurovascular aneurysms *in vivo*¹⁻². Reticulation of these foams has also shown varying clotting times *in vivo*, thus, varying the reticulation parameters with an automatic system could result in an optimal reticulation setting for the fastest occlusion of intracranial saccular aneurysms. This study will characterize SMP foams reticulated in new ways, and possibly provide insights for new applications for SMP foams, such as aneurysm occlusion devices and wound-healing tissue scaffolding applications. A unique property of SMP foams that make them useful medical devices is their ability to deform into a secondary shape and then revert back to its original geometry after actuation by heat, laser, or chemical species. Figure 1 gives a summary of the shape memory process.

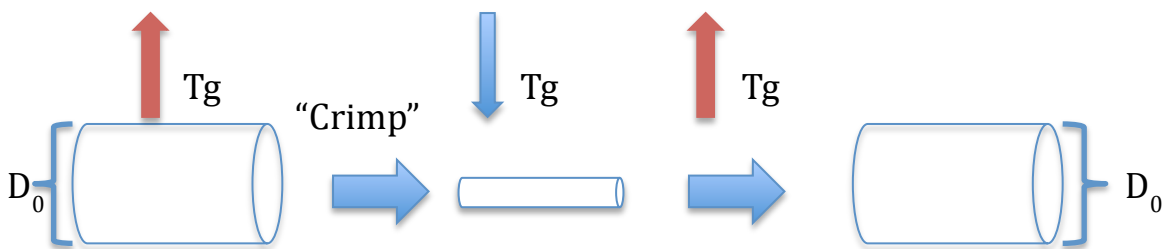


Figure 1: The concept of shape memory. The figure above graphically describes the shape recovery of a shape memory polymer. In order to “program” a shape memory polymer from its original geometry (D_0) into a secondary shape, the polymer must be heated to or above its glass transition temperature (T_g), then it can be manipulated into a secondary geometry, one in which it will reside once cooled below T_g . The original geometry can be recovered by heating the deformed polymer to or above T_g and allowing it to expand.

Clinical motivation

Intracranial aneurysms are weak spots within blood vessels in the brain that can swell into saccular aneurysms forming thin-walled balloon-like vessels that are susceptible to bursting. Bursting of these aneurysms may cause hemorrhagic stroke, which could result in paralysis or death. In the U.S, about 10 to 12 million people have a quiescent intracranial aneurysm³. Current treatment for these aneurysms include surgical clipping of the aneurysm and use of Guglielmi Detachable Coils (GDC) for occlusion of the aneurysm and endothelialization of the parent blood vessel, healing the aneurysm. There are drawbacks to both of these methods. Surgical clippings are effective treatment methods, but require a craniotomy and may have unwanted complications. GDC coils are the minimally invasive gold standard of treatment for aneurysms since they can access the aneurysms by a small incision in the iliac artery and insertion of the device by means of a microcatheter. Although minimally invasive, GDC coils have been shown to occasionally reopen after treatment, exposing the patient to a risk of recurrent hemorrhage⁴⁻⁵. SMP foams address some of the pitfalls of GDC coils and surgical clippings, by means of a minimally invasive treatment, aneurysm geometry conformation, and biocompatibility^{1-2,4-5}.

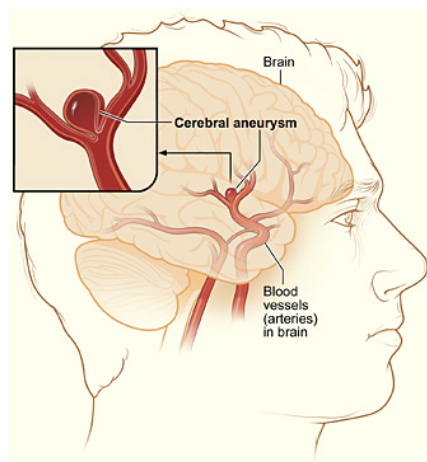


Figure 2: Illustration displaying a potential anatomical location of an intracranial aneurysm.

After initial fabrication, SMP foams are closed-celled structures, which inhibits infiltration of clotting factors, preventing the complete healing of an aneurysm⁶. Mechanical reticulation of SMP foams is a process that creates a network of open-celled pores within SMP foam while preserving the backbone framework of the foam². This process provides interconnected pathways for the accumulation of clotting factors and eventual thrombus formation within the bulk volume of the material, an important step in the healing process. Done manually, mechanical reticulation of SMP foams is a tedious process that requires a heavy investment of labor. Using an automatic system has reduced the required man-hours to reticulate SMP foams to about a twelfth of the original required time.

The performance, stability and healing time of a foam within an aneurysm, will depend upon the density and interconnectivity of open-celled pores, which influences the permeability, mechanical properties, and possibly volume recovery for SMP foams⁷⁻⁹. The accumulation of clotting factors is important as thrombus formation and filling of the aneurysm depends upon the availability of open-celled pathways within the foams. However, flow stagnation, resulting from a decreased permeability, may help to induce thrombogenesis within the aneurysms. Therefore, an optimum amount of reticulation would allow for infiltration and stagnation of clotting factors for the fastest aneurysm occlusion and healing within patients; future computational models and *in vivo* studies could verify this statement.

Varying open-celled densities may result in SMP foams with different mechanical properties, such as altered strength of SMP foams, characterized by the foam's resistance to compression. Knowing the compression strength of SMPs could be a potential way of estimating how well the

foam maintains its structural stability after mechanical reticulation with regards to the destruction of backbone struts within the foam. An important part of this research will be to verify whether certain amounts of open-celled pathway densities within SMP foams are feasible within the human body and for mass production. In this sense, the foams should not lose structural integrity when inserted within the body and the homogeneity of reticulated foams should be substantial enough that a section from one foam closely matches that of a section from another foam.

Biomedical motivation

This study would like to provide the research that could be the foundation for the use of SMP foams as tissue engineering scaffolds or wound healing devices. Similar materials, porous with a foamy nature, have been used as scaffolds to create suitable microenvironments for the integration of cells and growth factors for damaged tissues. Reticulated, open-celled, polyurethane SMP foams may provide an adequate environment for cell culturing, as the pathways created by reticulation of these foams could provide the appropriate environment for nutrient, oxygen, and waste diffusion⁹. This application of SMP foams would benefit traditional tissue engineering methods, as well as possibly accommodating future methods that utilize biological factors, such as bioactive cues for cells to respond to their environment, in the creation of tissue engineering scaffolds¹⁰. Tissue engineering scaffolds act as a function of scaffolds that maintain structural integrity and porous medium capable of improved biofactor, things such as proteins, genes, or cells, for delivery¹¹. That said, if there is an increased rate of biofactor delivery with larger porosity, it is more likely that the mechanical properties of the scaffold will be compromised¹¹. According to these criteria, there should be a certain degree of reticulation that would be optimal for creating a tissue engineering scaffold out of SMP foams, one with the

optimal porosity for biofactor delivery while not compromising mechanical properties¹². Changing the density of open-celled pores within the foams may provide the foam with a host of new tissue engineering applications, from use in the spine to dermal healing. This thesis will investigate the possibility of the application of SMP foams as tissue engineering scaffolds and suggest future work to validate this application.

CHAPTER II

METHODS

To study the effects of automatic mechanical reticulation, a protocol was followed to synthesize and process polyurethane SMP foams for testing of porous media and mechanical properties of the foams. The degree of reticulation was the only variable changed in the creation of samples for testing. Changes in the porous media properties and mechanical properties of SMP foams due to the degree of reticulation of foams with similar pore sizes and identical chemical composition were evaluated using various testing equipment.

Scanning electron microscope imaging of SMP foams

A scanning electron microscope was used to image the surface of reticulated and cleaned foams, giving a qualitative measure of the degree of reticulation. A series of four 5 mm slices of foam, resulting in five layers of foam, were taken from each sample to be imaged. This series of sliced foams was used in order to qualitatively assess how much reticulation occurred at each layer of the foam, and if there were any signs of structural damage within the foam. One image was taken of each foam shown in Table 1 and was used for qualitative comparison.

SMP foam fabrication, reticulation, and processing

Polyurethane SMP foams, fabricated using a method indicated by Singhal et al¹³, were cut with a Proxxon Thermocut into rectangular prisms measuring 2.5 cm X 6 cm X 7 cm or less for reticulation. Once cut, these rectangular pieces of foam were placed and secured on the tray of the automatic reticulation system.

Reticulation of prefabricated SMP foams was performed using the electromechanical system shown in Figure 2. This system consisted of a 30V precision variable DC power source, Parker 6K4-NK 4-axis stepper motor controller, three Gemini GT-L5 micro-stepping drives, three ES22B-DNR10 Stepper motors, a Danaher Z stage, and a Parker 404XR Series Slide, consisting of a X and Y stage. The interface between the SMP foam and the system consisted of a metal scaffold that held pins that reticulated SMP foams. The foams would lie upon a 110V Dental Lab Shaker, which would shake with its dial turned to its lowest setting and the switch set to Low Shake.

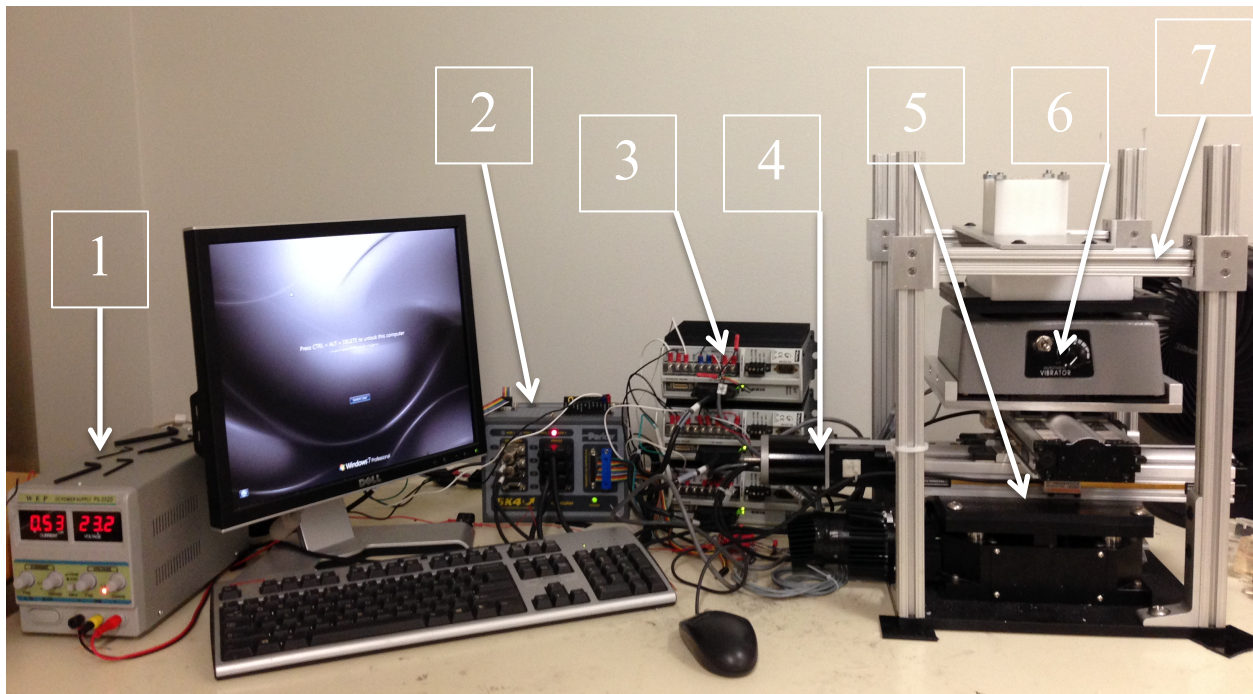


Figure 3: Image of the complete and assembled electro-mechanical system used to reticulate polyurethane shape memory polymer foams. 1) DC power supply that powered the system's drivers (3). 2) Parker 6K4-NK 4-axis stepper motor controller, communicated with the computer, which used Motion Planner software and coordinated the three drivers (3) to activate the motors (4). 3) Three Gemini GT-L5 micro-stepping drives which controlled the stepper motors of the system (4). 4) Stepper motors, which moved the stages of system (5). 5) Stages used to adjust the position of the foam. 6) Dental shaker used to shake the foam during reticulation. 7) Metal casing used to hold pins, which physically created pathways within SMP foams.

The electromechanical system shown in Figure 2 was operated using a program called Motion Planner. This program controlled the step size of the system, the step size being how far the X or Y stage moved after the Z stage had risen and reticulated the foam on the shaker. Physical constraints of this system were based upon the distance of displacement along the z-axis and the size of the pin holding setup above the foam tray. Therefore, the foams had to measure, at max, 6cm by 7cm by 2.5cm, with 2.5cm being the maximum thickness of the foams.

Four different levels of reticulated foams were created, each categorized by the size of the step taken by the stage, which held the designated SMP foam in place. Therefore, a 250um stage step size was referred to as a 250um reticulated foam. The degrees of reticulation were the following: 250um, 500um, 750um, and 1000um. A control was also used in order to measure the effect of reticulation against a baseline value. Table 1 shows the varying degrees of reticulation, what experiments will be performed for each reticulation level, and how many samples of each type of foam will be used for each experiment. Compression DMA is unique in that only extremes of reticulation, most and least reticulated, were tested and then compared.

Table 1: Proposed Independent Variables And The Number Of Samples To Use On Each Test

Independent Variables	SEM Imaging (# of samples)	Permeability (# of samples)	Compression DMA (# of samples)	Volume Expansion (# of samples)
Control	3	5	5	5
250 um	3	5	5	5
500 um	3	5	0	5
750 um	3	5	0	5
1000 um	3	5	0	5

Once cut and reticulated, the SMP foams had to undergo a cleaning process, which involved hydrochloric acid, isopropyl alcohol, and detergent (Contrad, VWR). This process was explained by Rodriguez et al in a previous study of manual reticulation of SMP foams².

Average pore size verification

A slice of each SMP foam sample used in permeability testing was taken and the average pore size of the foam was verified to ensure that each foam had similar average pore sizes. This was necessary in order to ensure that the permeability would not vary, based solely off of differences in average pore size of foams tested. Using a Leica long-range microscope with Jenoptic camera system, light microscope images of the various foams were taken. The average pore size of the foams was verified by using ImageJ software. For each foam sample, fifty different pore sizes were taken and then averaged. Equation 2 was used to calculate pore sizes.

$$\text{Pore Size} = \frac{\pi}{4} d^2 \quad \text{Equation (1)}$$

Permeability system testing of SMP foams

In order to characterize the porous media properties, permeability and form factor, of SMP foams, the permeability system and method of operation described by Muschenborn et al was used⁷. Permeability is defined as a value inversely proportional to the surface area of contact between the porous matrix and the fluid flow, while form factor is proportional to the projected cross-sectional area of the obstructing matrix perpendicular to the flow direction, both of which make up the porous media properties⁷. A 16 mm diameter biopsy punch was used to extract cylindrical compositions from parent slices of foams. Once extracted, these cylindrical foam samples were heated and slightly crimped down to 14 mm diameter, and were then inserted and

glued into a cylindrical foam sample chamber measuring 15 mm in diameter. This chamber was then inserted into a larger chamber, made of aluminum rather than poly(methylmethacralate) polymer as was previously used by Muschenborn et al⁷, which would measure the pressure difference along the porous medium sample. Once the larger chamber was properly in place, the *in vitro* closed loop flow system was allowed to run, measuring the pressure difference across the foam. Using the Forchheimer-Hazen-Dupuit-Darcy (FHDD) equation, the permeability and form factor of each reticulated sample could be calculated by measuring the pressure gradient measured across the foam in the flow chamber as a function of eight different Darcy velocities.

$$-\frac{\partial P}{\partial x} = \frac{\pi}{K} v_0 + \rho C v_0^2 \quad \text{Equation (2)}$$

Volume expansion of SMP foams

To understand the effects of reticulation on foam actuation properties of the SMP foams, volume expansion experiments were run on five samples of each degree of reticulated foam. This test was done by crimping five cylindrical SMP foams with 4 mm diameters and a length of 0.5 mm down to the smallest possible diameter, about 0.6 mm, over a 0.010” diameter piece of nitinol wire using a SC150-42 Stent Crimper (Machine Solutions, Inc.). Once crimped into its secondary geometry, the SMP foam was then held taught by the plate shown in Figure 4.



Figure 4: Volume actuation stability plate. The plate used to hold the foams upon the wire used to perform SMP foam actuation experiments.

Once attached, the plate and SMP foam were submerged into a water bath (Water bath, VWR) at 50 °C, with a thermocouple used to verify the temperature at every time interval. Immediately after the plate was submerged, a picture was taken of the foam. After an hour had passed, a picture was taken of the fully expanded SMP foam. The water bath setup can be seen in Figure 5.

The pictures taken of the foam were analyzed using ImageJ software. The images, from first submersion in the water to the final picture taken, were measured to compare the starting diameter of the cylindrical foam to the ending diameter and the volume of the foam before crimping. Once this experiment was performed upon each foam sample, Equation 3 was used to calculate the volume expansion ratio of each sample, where D_r represents the recovered diameter and D_c represents the crimped diameter.

$$V_E = \left(\frac{D_r}{D_c}\right)^2 \quad \text{Equation (3)}$$

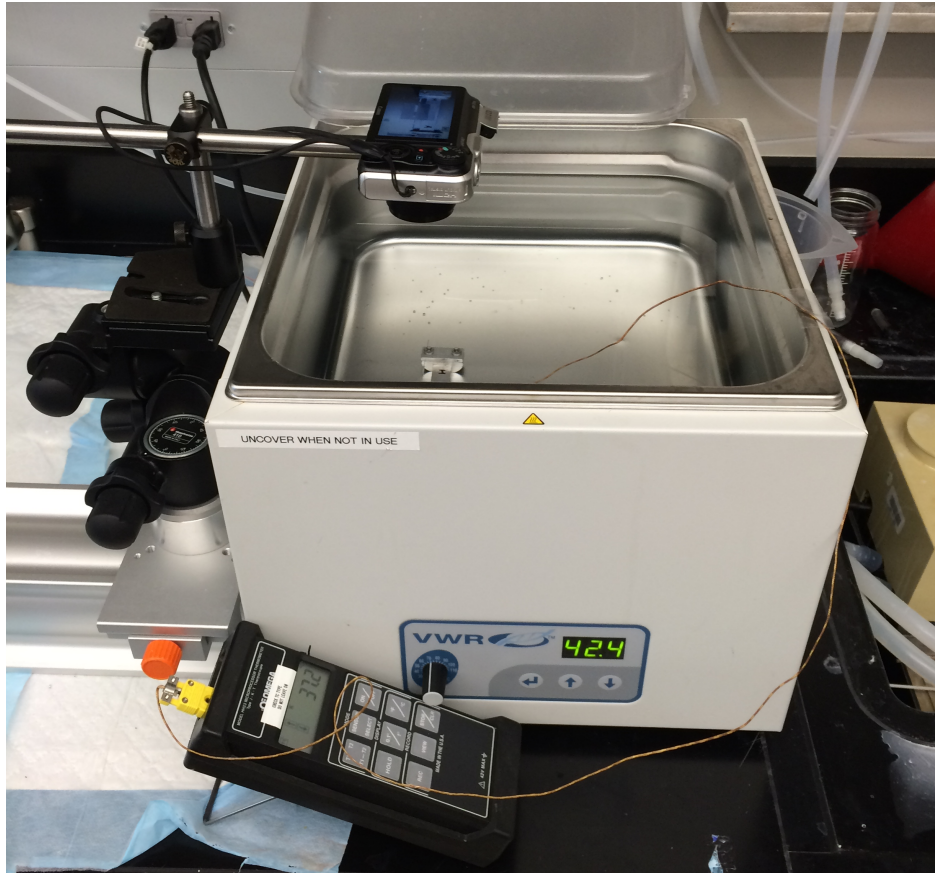


Figure 5: Volume actuation experimentation setup. Water bath, camera, stability plate, and thermocouple used to evaluate the actuation properties of differently reticulated SMP foams.

Characterization of SMP foams by dynamic mechanical analysis testing

Dynamic Mechanical Analysis (DMA) was used to evaluate the mechanical stability of the cleaned and reticulated SMP foams. A DMA system (Q800, TA Instruments) measured the mechanical stability of the SMP foams by means of a compression clamp attached to the DMA. Foams were cut into 15 mm diameter and 5 mm height cylindrical foams and were then inserted into the compression clamps of the DMA system. The system used a method consisting of a strain rate of 3% per minute, which measured the stress required to achieve 50% strain of each foam sample.

CHAPTER III

RESULTS AND DISCUSSION

Bulk SMP foam comparisons

The first comparison that could be made between the foams is shown in figure 6, the differences between varying foams and their reticulation levels. All of the foams were able to be processed except for the 250um step foam, shown in figure 7.

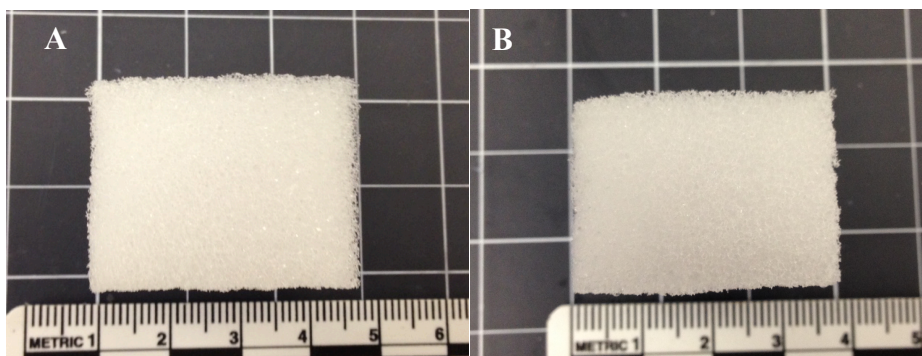


Figure 6: Image of a SMP foam post-fabrication and before reticulation (A) and after 500um reticulation (B).

Figure 6 shows there is not difference between pre-reticulation and post-reticulation, therefore, SEM imaging is needed to identify the effect of reticulation on the foams. The image of the 250um reticulated foam, shown in figure 7, was the first result of this thesis. It established an upper limit to reticulation by means of current foam processing methods.



Figure 7: Image of 250um step foam that was unsuccessfully processed. This was the first result of my thesis. From this, there is an established upper limit for the amount of reticulation possible by means of the current foam processing method.

SEM images of different degrees of reticulated foams

Shown in Figure 8 are the pictures of the SEM images of the foams cut into five pieces, separating them into a top, secondary, tertiary, penultimate, and bottom layers of foam. This enables the qualitative viewing of the extent of reticulation within a single foam. Figure 8 shows the progression of less reticulated foam to more reticulated foam, going from non-reticulated along the left column to 500um reticulated foam along the right column.

The non-reticulated foam can be seen to contain no open-celled pathways, as all of the membranes created from the foaming process are still intact. The most reticulated foam, 500um, appears to be evenly reticulated throughout with little spaces with membranes from reticulated foams. Also, from first glance, it seems that the 500um-reticulated foam does not have any broken struts in the pictures, which would have occurred from the process of reticulation. This is good for the mechanical stability of the foam, as the removal of struts would most likely hurt the structural integrity of the foams, leading to reduced mechanical strength.

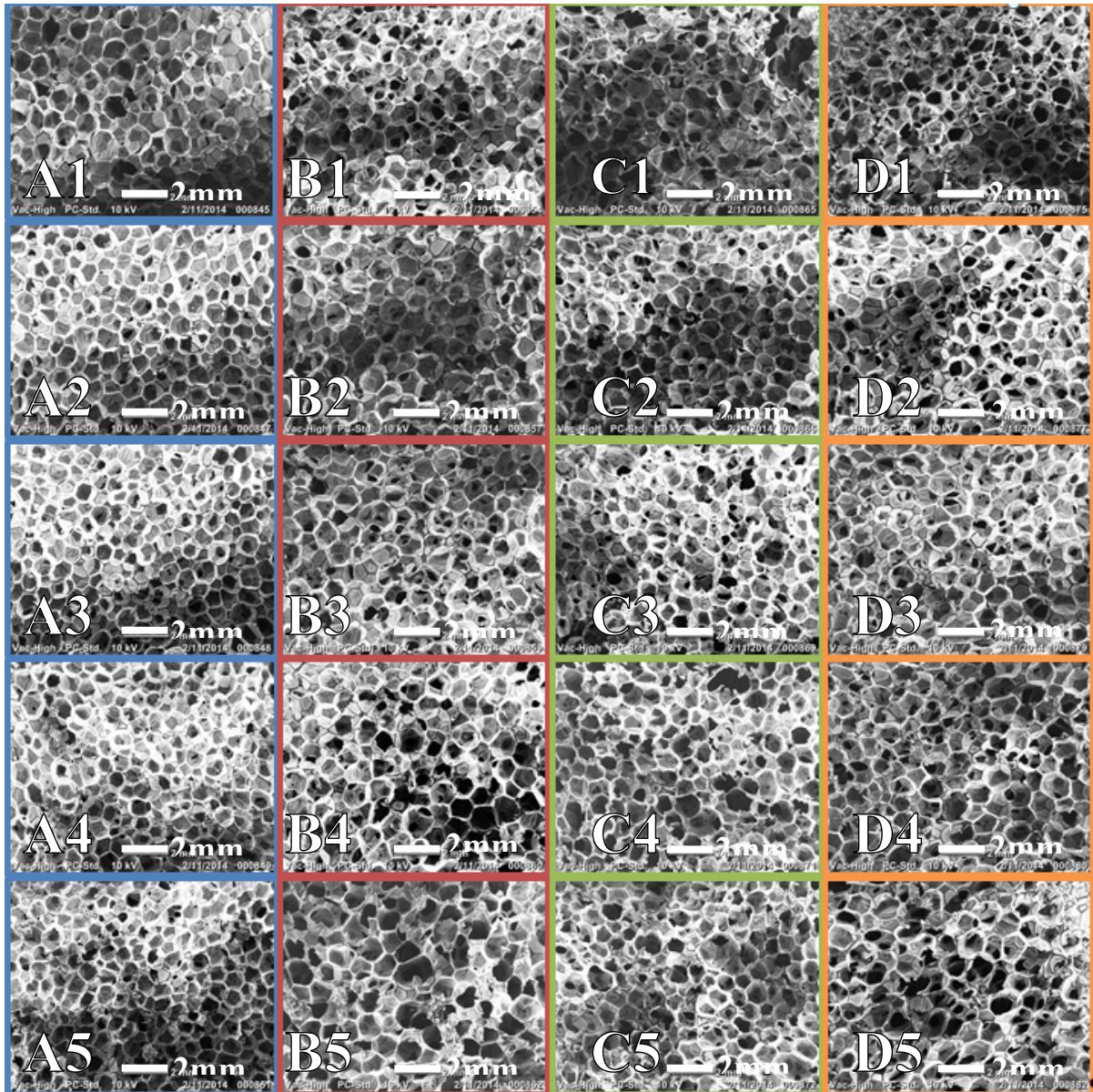


Figure 8: Matrix of SMP foams reticulated at varying rates and viewed at different depths with a scale at 2mm. The control, non-reticulated, foam is along the left column labeled A, the 1000um is next labeled B, then 750um labeled C, and finally 500um to the right, labeled D. The foams were cut four times to isolate a top, second, middle, third, and bottom layer. This maps from the least reticulated foam along the left column to the most reticulated foam along the right column.

It is difficult to assess the differences between the various layers of SMP foams in figure 8, this is why it is necessary to further assess the foams by means of their porous media properties.

Average pore sizes of tested SMP foams

Looking at Table 2, out of the three separately fabricated foams. From the sample of three foams used, there is a small standard deviation of .009mm from the average pore size of 0.17mm. These foams were used for permeability testing, as well. These results indicate that if there was any large deviation of permeability or form factor values, it was not due to the difference in average pore size of the foams⁷.

Table 2: List of the average pore sizes used for permeability testing.

<u>Foam Sample</u>	<u>Average Pore Size (mm)</u>
Foam 1	0.163
Foam 2	0.179
Foam 3	0.178

Permeability and form factor

Data used to calculate the Permeability and Form Factor are shown in figure 9. The permeability and form factor were calculated by measuring the pressure gradient across the SMP foam at eight different darcy velocities, the flow rate divided by cross sectional area. Figure 9 displays a graph of compiled pressure versus darcy velocity, data used to extrapolate Permeability and Form Factor.

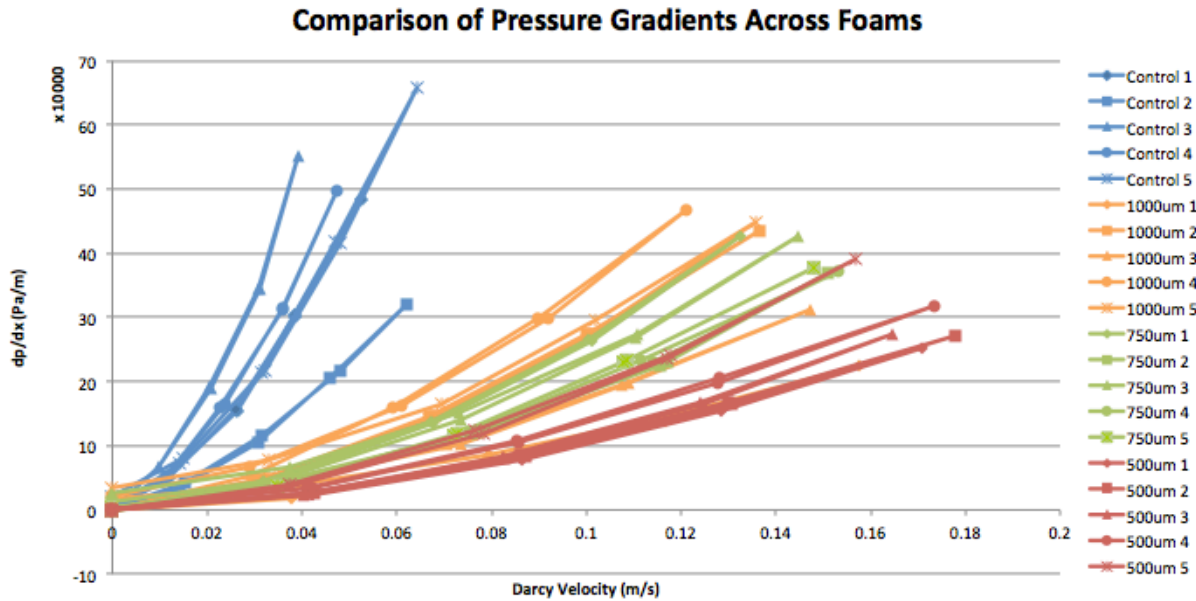


Figure 9: Graph of the Pressure gradient across the SMP foam as a function of the Darcy Velocity.

Figure 10 shows the permeability of the variously reticulated foams and the control foam and Figure 11 shows the form factor result of tested foams. According to Figure 10 and 11, with increasing amounts of reticulation, there is an increased value of permeability and decrease in form factor, with a significant difference between the control and reticulated samples and with less deviation between reticulated foams. The permeability results show that there is a correlation between an increase in the degree of reticulation and the permeability value. This outcome was expected, however the rate of the increase is subject to interpretation. It appears that there might be an exponential increase in the permeability corresponding to the degree of reticulation; however, future tests will be needed to validate this hypothesis.

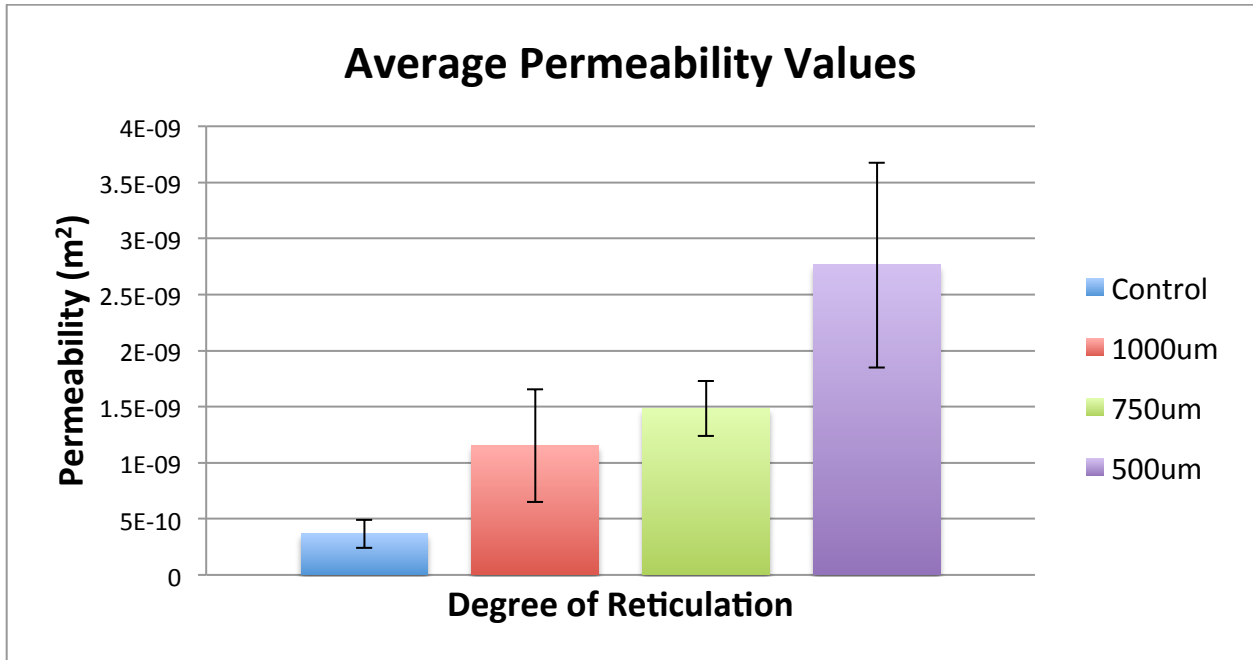


Figure 10: Permeability results as a function of the differential pressure. An increasing trend can be seen between the permeability and the degree of reticulation.

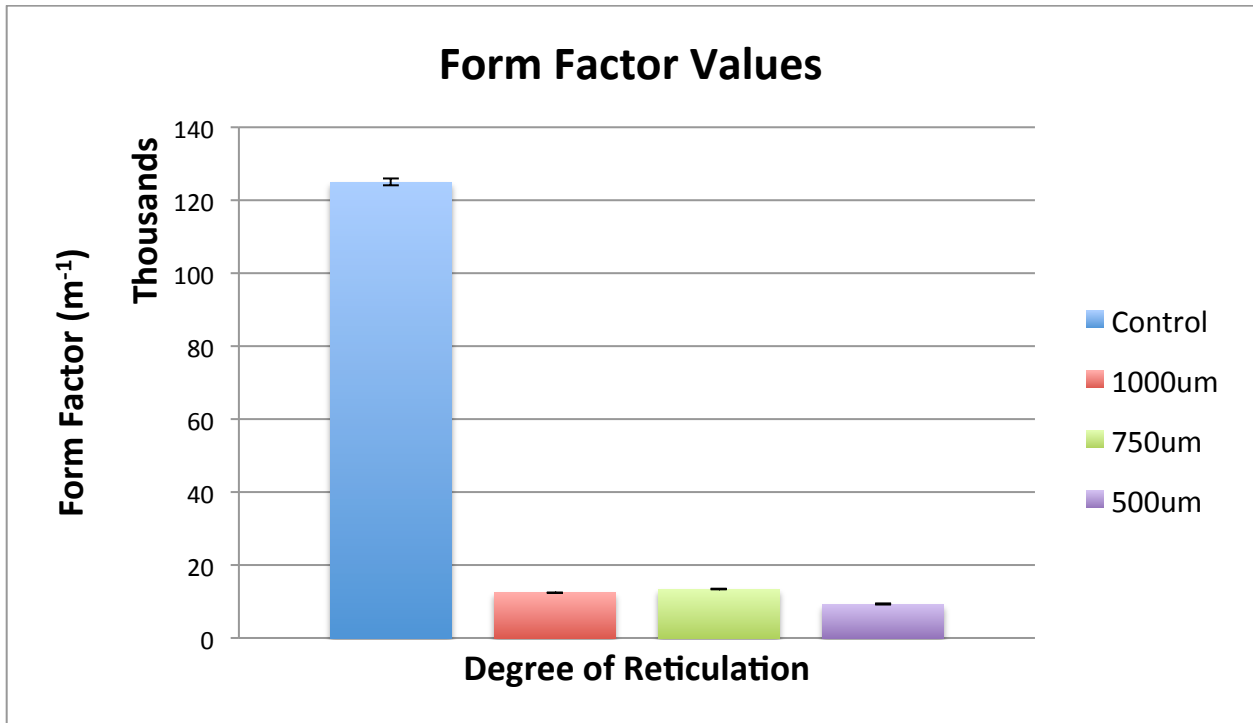


Figure 11: Plot of the form factor values for SMP foams reticulated to different degrees. There is a difference in an order of magnitude between the reticulated and non-reticulated foams. This

dramatic change is due to the clearing of membranes in the pores of the foams, reducing the amount of geometries impeding fluid flow in the foam.

The form factor results show a drop by an order of magnitude between the control foam and that of the reticulated foams. This steep drop is expected between reticulated and non-reticulated foams, as all reticulated foams lack membranes perpendicular to fluid flow. This means that in reticulated foams, the cross sectional area of obstructing matrix material was less in reticulated than it was in non-reticulated foams. This change in form factor could be seen by the SEM results, where membranes obstructing flow were cleared within reticulated foams.

Volume expansion of SMP foams

Figure 11 shows the results of the volume expansion experiments. The measurements for calculating the average diameter of the foam are shown in the table, with the average diameter and equation 3 used to calculate the average volume expansion of the SMP foams expanded in 50°C water. According to table 4, the control foam had the largest average expansion, and the 1000um had the least average expansion. This variation between the foams may be attributed to the variability between the foam samples used or where the samples were harvested from the foam, as a SMP foam is a fairly heterogeneous material.

Table 3: Table displaying average crimped diameter, expanded diameter, and volume expansion of SMP foams.

Foam Sample	Crimped Diameter (mm)	Expanded Diameters (mm)	Volume Expansion
Control	0.54 ± 0.01	3.86 ± 0.46	50.39 ± 12.13
1000um	0.57 ± 0.06	2.65 ± 0.15	21.81 ± 6.83
750um	0.68 ± 0.13	3.9 ± 0.2	33.03 ± 15.95
500um	0.73 ± 0.04	4.14 ± 0.27	32.09 ± 7.28

DMA results

A comparison of stress-strain tests for non-reticulated and 500um reticulated foam, which was used instead of 250um foam due to the inability to process 250um step foam, at ambient temperature is shown in Figure 12. The comparison between control foam and 500um foam was done in order to compare the mechanical stability of the least reticulated and most reticulated foams. The plot has a certain degree of variability in the rate at which a maximum stress is achieved and at what strain percentage. The control foams seemed to have a higher average maximum stress than the 500um compressed foams, but further testing and calculations need to be done in order to confirm that observation. These results seem to indicate that there is not a large difference in the structural stability between 500um foam and control foams. In itself, this result simply means that the foams may be compressed at similar forces. The rate at which each foam sample reaches maximum stress only slightly varies between the two differently processed foams.

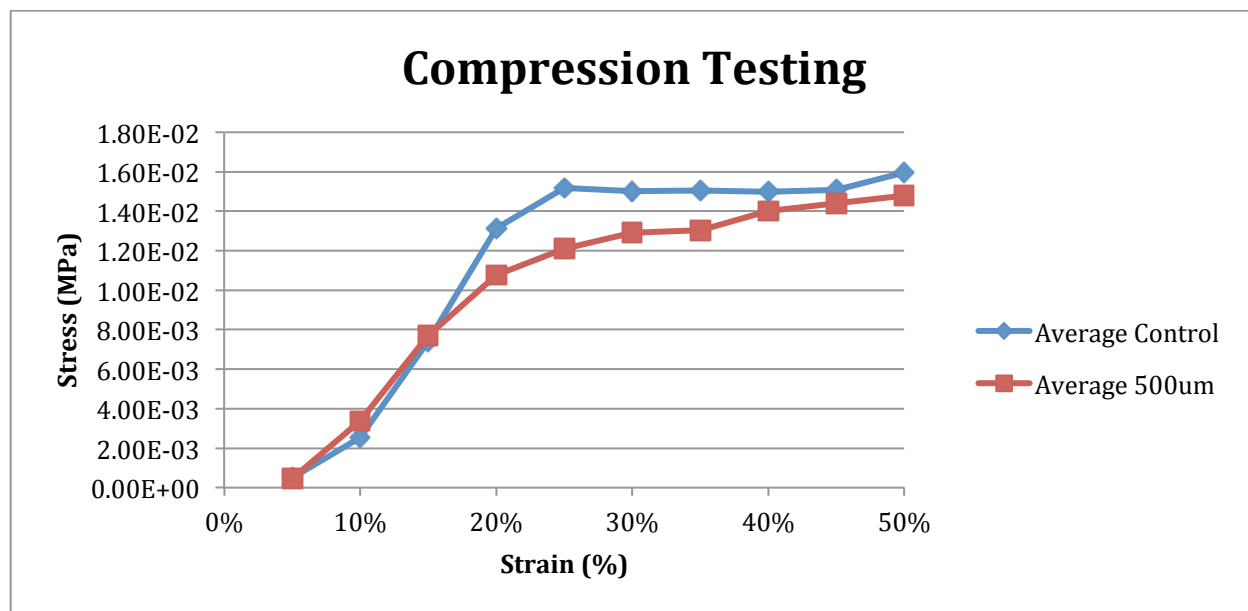


Figure 12: Plot of the stress-strain relationship between the average control and 500um reticulated SMP foam.

Discussion

Porous Media Properties

This study had two major results, increasing the degree of reticulation within foam samples increased the permeability of the foam and the use of an automated reticulation system produced consistent reticulated samples for study. In relation to the clinical motivation, the increase in permeability is helpful in fluid and clotting factor diffusion throughout the foam. The factors to consider when evaluating potential for aneurysm occlusion and healing are permeability, flow stagnation, and surface area for clotting factor adhesion. Permeability influences all three of these parameters, with permeability and flow stagnation negatively influencing each other^{7,11}. This study is unable to assess how well the reticulated foams induce flow stagnation or clotting factor adhesion, but future computational models, using the permeability values listed here may help to assess these two factors, effectively assessing the ability of reticulated SMP foam to

induce occlusion and aneurysm healing. Once flow stagnation and clotting factor adhesion have been assessed by computational models, *in vivo* studies may be performed based off the information from this study and that of the computational study.

Volume expansion and mechanical stability

Volume expansion tests demonstrated the affinity for reticulated foam to plasticize at a faster rate than non-reticulated foam at ambient room temperature and atmospheric water vapor. The volume expansion ratio between the final diameter and initial diameter demonstrated the degree of initial plasticization between reticulated foams and non-reticulated foams. From this, future medical devices must be stored in airtight containers with minimal water vapor before clinical implementation. Also, the 750um samples were a good example of the variability of the foam composition within a foam sample, as these samples may have been harvested from a more heterogeneous porous section of the foam, resulting in compromised shape memory recovery.

Mechanical stability was briefly evaluated with the maximum and minimum reticulation levels evaluated. The results may indicate that there was minimal damage to the struts within the 500um tested foams. This is a good result, as one of the desirable outcomes of reticulation is a foam sample that has the same structural stability as a non-reticulated foam sample.

CHAPTER IV

CONCLUSION

This study qualitatively and quantitatively observed the effects of varying the settings of an automated mechanical reticulation system by means of SEM imaging, permeability testing, volume expansion experiments, and mechanical stability testing. From a macro-scale view of the foams, reticulation does not appear to affect the foam, except for at extreme cases of reticulation. Aside from the top layers of foams, SEM imaging was not able to sufficiently differentiate the foams that have been reticulated, however they were good images to validate that the foam struts appeared to not be damaged after reticulation. The permeability results validated the hypothesis that increasing the amount of reticulation in foams increases the permeability of the SMP foams, as was indicated by Muschenborn et al⁷.

From the permeability results, there also seems to be a trend that increasing the step size by half exponentially increases the permeability of the foams that were reticulated, as could be seen between the 1000um, 750um, and 500um foams. More testing will need to be conducted to verify this hypothesis. The volume expansion experiments showed that all foams were capable of volume recovery to within a tenth of a millimeter of the original volume in 50°C water, but that the starting volume of the SMP foams varied in the testing. With the more reticulated foams having a larger starting volume, even though they were contained in an airtight container and followed the same procedure. This may mean that reticulating foams creates pathways for water vapor to penetrate the volume of the foam, as opposed to non-reticulated foams, which still had membranes to impede water vapor penetration within the foams. This water vapor penetration

has implications for the proposed device that would be used to treat intracranial aneurysms, as the device must be in an airtight container all the way up until implementation in the body, so as to preserve the device's shape memory effect. Once inside the body, reticulated foam may even start actuating faster, giving the device less time to get the device to an aneurysm before deployment.

The results will not be able to help future computation models to assess how well different levels of reticulation will be able to occlude intracranial aneurysms, but they do give an overview of the effectiveness of the device to create a desired degree of reticulation. Once computational models have been created and a theoretical optimal reticulation level has been determined, the automatic reticulation system will be capable of implementing the reticulated level indicated by computational models, which could then be used for animal studies to compare the rate of clot formation in intracranial aneurysms.

REFERENCES

1. Rodriguez JNC, F. J.; Wilson, T. S.; Miller, M. W.; Fossum, T.; Hartman, J.; Tuzun, E.; Singhal, P.; Maitland, D. J. In vivo tissue response following implantation of shape memory polyurethane foam in a porcine aneurysm model. *Journal of Biomedical Materials Research Part A* 2013.
2. Rodriguez JN, Miller MW, Boyle A, Yang C-K, Nash L, Wilson TS, Maisano JA, Skoog H, Maitland DJ: Biological interactions and effects of mechanical reticulation on shape memory polymer foams for vascular occlusion. *J Mech Behav Biomed* 2013, in preparation.
3. Burns JD, Huston J, Layton KF, Piepgras DG, Brown RD: Intracranial aneurysm enlargement on serial magnetic resonance angiography frequency and risk factors. *Stroke* 2009, 40:406-411.
4. Sluzewski M, van Rooij WJ, Slob MJ, et al. Relation between aneurysm volume, packing, and compaction in 145 cerebral aneurysms treated with coils. *Radiology* 2004;231:653–58.
5. Szikora I, Seifert P, Hanzely Z, et al. Histopathologic evaluation of aneurysms treated with Guglielmi detachable coils or matrix detachable microcoils. *AJNR Am J Neuroradiol* 2006;27:283–8.
6. Metcalfe, A.; Desfaits, A.-C.; Salazkin, I.; Yahia, L. H.; Sokolowski, W. M.; Raymond, J. of *Biomaterials* 2003, 24, 491.
7. Muschenborn AD, Ortega JM, Szafron JM, Szafron DJ, Maitland DJ: Porous media properties of reticulated shape memory polymer foams and mock embolic coils for aneurysm treatment. *Biomedical Engineering Online* 2013, p 5-12.
8. Hwang, W., B.L. Volk, F. Akberali, P. Singhal, J.C. Criscione, & D.J. Maitland. Estimation of Aneurysm Wall Stresses Created by Treatment with a Shape Memory Polymer Foam Device. *Biomechanics and Modeling in Mechanobiology*, pp. 715-729, May 2012
9. Humphrey JD, Na S (2002) Elastodynamics and arterial wall stress. *Ann Biomed Eng* 30(4):509–523. doi:10.1114/1.1467676
10. Chan, B. P., and K. W. Leong. "Scaffolding in tissue engineering: general approaches and tissue-specific considerations." *European spine journal* 17.4 (2008): 467-479.
11. Qiu Li Loh and Cleo Choong. *Tissue Engineering Part B: Reviews*. December 2013, 19(6): 485-502.

12. Hollister, Scott J. (2005) Porous scaffold design for tissue engineering. *Nature Materials*, p 518-524.
13. Pooja Singhal, Ward Small, Elizabeth Cosgriff-Hernandez, Duncan J. Maitland, Thomas S. Wilson, Low density biodegradable shape memory polyurethane foams for embolic biomedical applications, *Acta Biomaterialia*, Volume 10, Issue 1, January 2014, Pages 67-76